

Schur-type preconditioning of a phase-field fracture model in mixed form

Timo Heister¹, Katrin Mang^{2,*}, and Thomas Wick²

¹ Clemson University, Martin Hall, Clemson, SC 29634, USA

² Leibniz Universität Hannover, Institute of Applied Mathematics, Welfengarten 1, 30167 Hannover, Germany

In the context of phase-field modeling of fractures in incompressible materials, a mixed form of the elasticity equation can overcome possible volume locking effects. The drawback is that a coupled variational inequality system with three unknowns (displacements, pressure and phase-field) has to be solved, which increases the overall workload. Efficient preconditioning at this point is an indispensable tool. In this work, a problem-specific iterative solver is proposed leveraging the saddle-point structure of the displacement and pressure variable. A Schur-type preconditioner is developed to avoid ill-conditioning of the phase-field fracture problem. Finally, we show numerical results of a pressure-driven benchmark which to confirm the robustness of the solver.

© 2021 The Authors. *Proceedings in Applied Mathematics & Mechanics* published by Wiley-VCH GmbH.

1 Introduction

Phase-field fracture emerged from a variational formulation introduced in [1,2] and is an attractive model approach to simulate crack propagation in solid materials. Classical phase-field fracture modeling in nearly incompressible materials will cause locking effects, i.e., the values of the displacement field are underestimated. With help of a mixed form we get a stable problem formulation up to the incompressible limit [3]. For details on the phase-field fracture model in mixed form, we refer to [4]. A Galerkin finite element discretization with three unknowns $U := (u, p, \varphi)$ yields a nonlinear system of the form $\mathcal{M}U = F$ with a block 3×3 matrix $\mathcal{M} \in \mathcal{R}^{n \times n}$, U and $F \in \mathcal{R}^n$. For inf-sup stability a Taylor-Hood element Q_2^c/Q_1^c is used for the (u, p) system. We adapt Newton's method as a nonlinear solver. Inside, the linear system is non-symmetric and we use a GMRES (generalized minimal residual) method. Due to regularization parameters, various material parameters, and the spatial discretization parameter h , the problem is ill-conditioned and requires a preconditioner.

The main contribution of this work is a robust Schur-type preconditioner for this specific phase-field fracture problem in mixed form to allow numerical solution of fractures in incompressible materials. The mixed form of the elasticity equation has a saddle point structure, which allows to reuse spectral approximations for the inverse matrices from the Stokes problem [5,6].

2 Notation and problem setup

Let Ω be an open and smooth two-dimensional domain and T is a time interval. The lower-dimensional crack is approximated by a phase-field indicator function $\varphi : (\Omega \times T) \rightarrow [0, 1]$ with $\varphi = 0$ in the crack and $\varphi = 1$ in the unbroken area. The bandwidth of the zone between broken and unbroken is named ϵ . Further, a displacement function is defined as $u : (\Omega \times T) \rightarrow \mathcal{R}^2$. In the following, the scalar-valued L^2 -product is denoted by $(x, y) := \int_{\Omega} x \cdot y \, d\Omega$, whereas the vector-valued L^2 -product is described by $(X, Y) := \int_{\Omega} X : Y \, d\Omega$, with the Frobenius product $X : Y$ of two vectors X and Y . We define function spaces $\mathcal{V} := H_0^1(\Omega)^2$, $\mathcal{W} := H^1(\Omega)$ and a convex subset $\mathcal{K} := \mathcal{K}(\varphi^{n-1}) \subset \mathcal{W}$ and $\mathcal{U} := L_2(\Omega)$. Further, the degradation function is defined as $g(\varphi) = (1 - \kappa)\varphi^2 + \kappa$, where κ is a sufficiently small regularization parameter. The stress tensor is defined as $\sigma(u) := 2\mu E_{\text{lin}}(u) + \lambda \text{tr}(E_{\text{lin}}(u))I$ with a linearized strain tensor $E_{\text{lin}}(u) := \frac{1}{2}(\nabla u + \nabla u^T)$, material dependent Lamé coefficients λ and μ and the two-dimensional identity matrix I . The critical energy release rate is denoted as G_c . Based on this notation, the pressurized phase-field fracture model in its classical form can be formulated as follows [7]:

Problem 1 (Pressurized phase-field fracture in classical form) Let a (constant) pressure $\rho \in \mathcal{W}^{1,\infty}(\Omega)$ be given. Given the initial data $\varphi^{n-1} \in \mathcal{K}$. Find $u := u^n \in \mathcal{V}$ and $\varphi := \varphi^n \in \mathcal{K}$ for loading steps $n = 1, 2, \dots, N$ with $\{u, \varphi\} \in \mathcal{V} \times \mathcal{K}$ such that

$$\begin{aligned} (g(\tilde{\varphi})\sigma(u), E_{\text{lin}}(w)) + (\tilde{\varphi}^2 \rho, \nabla \cdot w) &= 0 \quad \forall w \in \mathcal{V}, \\ (1 - \kappa)(\varphi\sigma(u) : E_{\text{lin}}(u), \psi - \varphi) + 2(\varphi\rho\nabla \cdot u, \psi - \varphi) + G_c \left(-\frac{1}{\epsilon}(1 - \varphi, \psi - \varphi) \right. \\ &\quad \left. + \epsilon(\nabla\varphi, \nabla(\psi - \varphi)) \right) \geq 0 \quad \forall \psi \in \mathcal{K}. \end{aligned}$$

In the elasticity part, time-lagging $\tilde{\varphi} := \varphi^{n-1}$ is used in the phase-field variable φ to obtain a convex functional [8]. Following [4], we introduce a pressure $p := \lambda \text{tr}(E_{\text{lin}}(u))$ and arrive at:

* Corresponding author: e-mail mang@ifam.uni-hannover.de, phone +49 511 762 2336



This is an open access article under the terms of the Creative Commons Attribution-NonCommercial-NoDerivs License, which permits use and distribution in any medium, provided the original work is properly cited, the use is non-commercial and no modifications or adaptations are made.

Problem 2 (Pressurized phase-field fracture in mixed form) Let $\rho \in \mathcal{W}^{1,\infty}(\Omega)$ be given. Given the initial data $\varphi^{n-1} \in \mathcal{K}$. Find $u := u^n \in \mathcal{V}$, $p := p^n \in \mathcal{U}$ and $\varphi := \varphi^n \in \mathcal{K}$ for loading steps $n = 1, 2, \dots, N$ with $\{u, p, \varphi\} \in \mathcal{V} \times \mathcal{U} \times \mathcal{K}$ such that

$$\begin{aligned} & \left(g(\tilde{\varphi})\sigma(u, p), E_{\text{lin}}(w) \right) + (\tilde{\varphi}^2 \rho, \nabla \cdot w) = 0 \quad \forall w \in \mathcal{V}, \\ & g(\tilde{\varphi})(\nabla \cdot u, q) - \left(\frac{1}{\lambda} p, q \right) = 0 \quad \forall q \in \mathcal{U}, \\ & (1 - \kappa)(\varphi\sigma(u, p) : E_{\text{lin}}(u), \psi - \varphi) + 2(\varphi\rho\nabla \cdot u, \psi - \varphi) + G_c \left(-\frac{1}{\epsilon}(1 - \varphi, \psi - \varphi) + \right. \\ & \quad \left. \epsilon(\nabla\varphi, \nabla(\psi - \varphi)) \right) \geq 0 \quad \forall \psi \in \mathcal{K}, \end{aligned}$$

where the stress tensor is now defined as $\sigma(u, p) := 2\mu E_{\text{lin}}(u) + pI$.

3 Schur-type preconditioner of a phase-field fracture model in mixed form

Instead of solving the arising linear system $\mathcal{M}U = F$ directly, we apply right preconditioning [9] to reduce the condition number of the system. The system matrix \mathcal{M} of the mixed phase-field fracture in Problem 2 has the following block structure:

$$\mathcal{M} = \begin{pmatrix} M^{uu} & M^{up} & M^{u\varphi} \\ M^{pu} & M^{pp} & M^{p\varphi} \\ M^{\varphi u} & M^{\varphi p} & M^{\varphi\varphi} \end{pmatrix} = \begin{pmatrix} g(\tilde{\varphi})A & g(\tilde{\varphi})B^T & 0 \\ g(\tilde{\varphi})B & -\frac{1}{\lambda}M_p & 0 \\ E & F & L \end{pmatrix}, \quad P = \begin{pmatrix} g(\tilde{\varphi})A_u & g(\tilde{\varphi})B^T & 0 \\ 0 & S & 0 \\ 0 & 0 & L \end{pmatrix},$$

where $S = -\frac{1}{\lambda}M_p - g(\tilde{\varphi})B^T \cdot [g(\tilde{\varphi})A]^{-1} \cdot g(\tilde{\varphi})B$ is the Schur complement. Block A is the mass matrix of the displacement, B and B^T are symmetric off-diagonal blocks coupling u and p , and M_p is the mass matrix of the pressure variable. The blocks E , F and L contain the entries coming from the phase-field equation, where L is Laplacian-like. The approximated inverse of the designed preconditioning matrix P is

$$P^{-1} \approx \begin{pmatrix} \frac{1}{g(\tilde{\varphi})}(\tilde{A})^{-1} & -(\tilde{A})^{-1}B^T\tilde{S}^{-1} & 0 \\ 0 & \tilde{S}^{-1} & 0 \\ 0 & 0 & \tilde{L}^{-1} \end{pmatrix}, \quad \tilde{S}^{-1} = -\left(\left(\frac{1}{\lambda} + \frac{1}{2\mu} \right) (\phi_j^p, \phi_i^p) \right)^{-1}.$$

The approximation \tilde{S}^{-1} via a mass matrix of the pressure field is spectrally equivalent to S^{-1} [10]. Here, $\{\phi_i^p\}$ are the basis functions of the pressure space. For the incompressible limit $\nu = 0.5$ the Schur complement approximation becomes $\tilde{S}^{-1} = -\left(\frac{1}{2\mu} (\phi_j^p, \phi_i^p) \right)^{-1} = -2\mu \left((\phi_j^p, \phi_i^p) \right)^{-1}$. With spectrally equivalent \tilde{A} and \tilde{S} of A and S , respectively, the condition number of MP^{-1} is independent of h .

4 Numerical results

In the following, the numerical solution strategy of Problem 2 is explained. Afterwards, numerical tests allow to evaluate the performance of the newly developed preconditioner for a two-dimensional pressure-driven fracture derived from Sneddon [11], and Sneddon and Lowengrub [12].

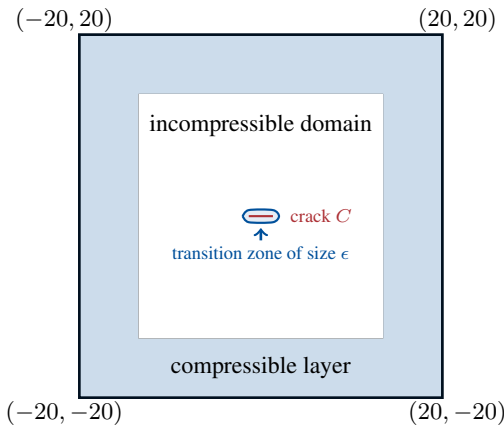
4.1 Numerical solution strategy

For the spatial discretization of Problem 2, we employ a Galerkin finite element method in each incremental step, where the domain Ω is partitioned into quadrilaterals. To fulfill a discrete inf-sup condition, stable Taylor-Hood elements with bi-quadratic shape functions (Q_2^c) for the displacement field u and bilinear shape functions (Q_1^c) for the pressure variable p and the phase-field variable φ are used as in [4]. In the classical problem formulation (Problem 1), $Q_1^c Q_1^c$ elements are typically used for the (u, φ) system. For a fairer comparison with the mixed form, we use higher order $Q_2^c Q_1^c$ elements also for the classical form.

The crack irreversibility is treated with a primal-dual active-set method [13]. As a linear solver GMRES is used with the Schur-type preconditioner from Section 3 with a relative tolerance of 10^{-5} . Therein, the blocks \tilde{L}^{-1} and \tilde{S}^{-1} are approximated by one cycle of Algebraic Multigrid. For the block $(g(\tilde{\varphi})\tilde{A})^{-1}$ a Conjugate Gradient method (CG) is used with a relative tolerance of 10^{-6} which is preconditioned as well by one cycle of Algebraic Multigrid. The base of the implementation is documented in [14]. This project is embedded in deal.II [15], which offers scalable parallel algorithms for finite element computations. The deal.II library in turn uses functionalities from other libraries such as Trilinos [16], including ML which we use as the Algebraic Multigrid preconditioner.

4.2 Test case: Sneddon’s layered benchmark

As a test case, the pressure-driven cavity from [17] is modified similar to [3]. We work in a two-dimensional domain $\Omega = (-20, 20)^2$. We add a compressible layer of size 10 around the incompressible domain to allow deforming of the solid on a finite domain. A sketch of the geometry and the setting of numerical and material parameters is given in Figure 1. In this domain, an initial crack with length $2l_0 = 2.0$ and thickness h of two cells by help of the phase-field function φ , i.e., $\varphi = 0$ in the crack and $\varphi = 1$ elsewhere. As boundary conditions, the displacements u are set to zero on $\partial\Omega$. For the phase-field variable, we use homogeneous Neumann conditions, i.e., $\epsilon\partial_n\varphi = 0$ on $\partial\Omega$. The mesh around the initial crack is prerefined geometrically. In all results, the total number of degrees of freedom ($\#dof$) on the whole domain is listed in the following.



parameter	description	value
Ω	domain	$(-20, 20)^2$
h	cell diameter	0.088 to 0.011
ϵ	length-scale	$2h$ or 0.176
κ	regularization parameter	10^{-4}
l_0	half crack length	1.0
G_c	critical energy release rate	1.0
E	Young’s modulus	1.0
ν	Poisson ratio	0.2 and 0.5
ρ	constant pressure in the crack	10^{-3} Pa
$\#Newton/AS$	allowed number of Newton iterations	30
TOL_{AS}	Newton tolerance	10^{-7}
$\#line\ search$	allowed number of line search steps	10

Fig. 1: Left: geometry of the two-dimensional Sneddon’s test with a compressible layer of size 10. Right: parameter settings of Sneddon’s layered benchmark. The size of the minimal cell diameter h , the crack width ϵ and the Poisson ratio vary depending on the test case. All the other parameters are kept fixed.

formulation	h	ϵ	$\#dof$	$\emptyset GMRES$	$\emptyset CG$	$\emptyset AS$	COD_{max}
classical	0.088	0.176	57, 733	4.50	21	8.75	0.00208593
classical	0.044	0.176	169, 621	5.00	25	13.75	0.00204217
classical	0.022	0.176	600, 613	5.75	30	25.25	0.00200234
classical	0.088	$2h$	57, 733	4.75	21	8.75	0.00208634
classical	0.044	$2h$	169, 621	4.25	25	15.75	0.00199855
classical	0.022	$2h$	600, 613	4.25	28	21.25	0.00194055
mixed	0.088	0.176	64, 184	5.50	21	9.25	0.00216240
mixed	0.044	0.176	188, 504	5.00	26	13.25	0.00212127
mixed	0.022	0.176	667, 384	6.00	32	24.75	0.00208372
mixed	0.088	$2h$	64, 184	5.50	21	9.25	0.00216302
mixed	0.044	$2h$	188, 504	5.25	27	15.50	0.00204751
mixed	0.022	$2h$	667, 384	6.75	31	20.25	0.00197197
reference [17]							0.00192

Table 1: Average number of GMRES iterations ($\emptyset GMRES$) per Newton/active set (AS) step, average number of the CG iterations ($\emptyset CG$) for $g(\varphi)A^{-1}$, average number of AS ($\emptyset AS$), and the goal functional crack opening displacement (COD_{max}) based on the classical model ($Q_2^c Q_1^c$ elements) or the newly developed mixed model ($Q_2^c Q_1^c Q_1^c$ elements) for different problem sizes and length scale ϵ for $\nu = 0.2$.

formulation	h	ϵ	$\#dof$	$\emptyset GMRES$	$\emptyset CG$	$\emptyset AS$	COD_{max}
mixed	0.088	$2h$	64, 184	27.25	20	4.75	0.00178519
mixed	0.044	$2h$	188, 504	13.50	30	7.75	0.00163546
mixed	0.022	$2h$	667, 384	10.00	39	10.75	0.00155880
reference [3]							0.0015

Table 2: Average number of GMRES iterations ($\#GMRES$) per Newton/active set (AS) step, average number of Newton/AS ($\#AS$), and goal functional COD_{max} based on the newly developed mixed model ($Q_2^c Q_1^c Q_1^c$ elements) for different problem sizes and setting of the length scale parameter ϵ for $\nu = 0.5$.

In Table 1, we report results for a compressible case ($\nu = 0.2$) with three different refinement levels for two types of elements: $Q_2^c Q_1^c$ finite elements based on the classical form of quasi-static pressurized phase-field fracture, and $Q_2^c Q_1^c Q_1^c$ finite elements (notated as ‘mixed’) based on Problem 2. Most important is the average number of GMRES iterations per active set

step and how they depend on mesh size h and ϵ . Furthermore, the average number of CG iterations for the approximation of $(g(\bar{\varphi})\hat{A})^{-1}$ as well as the average number of active set/Newton iterations are given. In the last column, the maximal crack opening displacement (COD) is given defined as

$$\text{COD}_{\max} := [u \cdot n](0) \approx \int_{-20}^{20} u(0, y) \cdot \nabla \varphi(0, y) dy. \quad (1)$$

The reference value for COD is given by Sneddon and Lowengrub [12], for $\nu = 0.2$ it is $\text{COD}_{\text{ref}} = 0.00192$, for $\nu = 0.5$ it holds $\text{COD}_{\text{ref}} = 0.0015$. In Table 1, we observe that the number of GMRES iterations is nearly constant in h and ϵ (second half of the table). This indicates robustness in h and the length scale ϵ for $\nu = 0.2$. COD_{\max} is slightly overestimated within the mixed model. Table 2 contains the results of the incompressible case based on Problem 2 with a Poisson ratio $\nu = 0.5$ which can not be computed with the classical model ($\lambda = \infty$). The number of GMRES iterations is decreasing with a finer mesh size, the average number of CG and active set iterations are similar to the previous test cases, and the values for COD_{\max} are promising. See Figure 2 for zoomed-in snapshots of the pressure field and the phase-field for the incompressible limit. The pressure field is naturally zero inside the crack and has its maximum values in the crack tips on the left and the right.

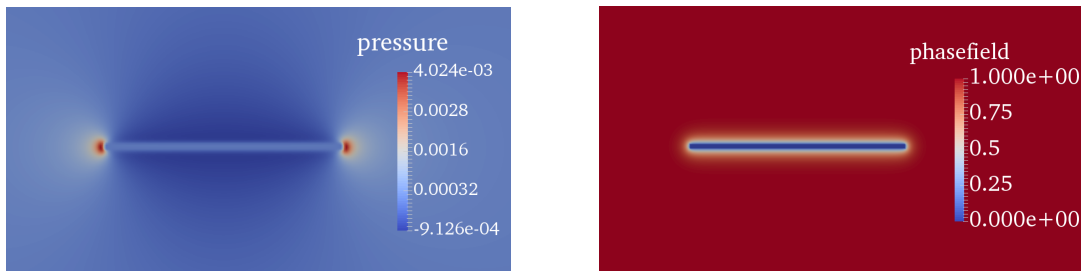


Fig. 2: Zoom-in snapshots of the crack area: the pressure field and the phase-field are depicted for $\nu = 0.5$ computed with $Q_2^c Q_1^c Q_1^c$ elements based on a mesh with two global and six local refinement steps ($d = 0.022$).

5 Conclusion

In this work, a robust preconditioner for a phase-field fracture model in mixed form is developed and tested on a pressure-driven phase-field fracture example. Robustness in the number of GMRES iterations with refinement was observed for the compressible tests with $\nu = 0.2$. In the incompressible case the number of GMRES iterations decreases with refinement and a smaller length scale ϵ .

Acknowledgements Open access funding enabled and organized by Projekt DEAL.

References

- [1] G. Francfort and J. J. Marigo, *Journal of the Mechanics and Physics of Solids* **46**(8), 1319–1342 (1998).
- [2] B. Bourdin, G. Francfort, and J. J. Marigo, *J. Mech. Phys. Solids* **48**(4), 797–826 (2000).
- [3] S. Basava, K. Mang, M. Walloth, T. Wick, and W. Wollner, arXiv preprint arXiv:2006.16566 (2020).
- [4] K. Mang, T. Wick, and W. Wollner, *Computational Mechanics* **65**(1), 61–78 (2020).
- [5] M. Benzi, G. H. Golub, and J. Liesen, *Acta numerica* **14**, 1–137 (2005).
- [6] D. Boffi, F. Brezzi, and M. Fortin, *Mixed Finite Elements, Compatibility Conditions, and Applications: Lectures given at the CIME Summer School held in Cetraro, Italy, June 26-July 1, 2006* p. 45 (2008).
- [7] T. Wick, *Multiphysics Phase-Field Fracture: Modeling, Adaptive Discretizations, and Solvers* (De Gruyter, 2020).
- [8] T. Wick, *SIAM Journal on Scientific Computing* **39**(4), B589–B617 (2017).
- [9] Y. Saad, *Iterative methods for sparse linear systems* (SIAM, 2003).
- [10] D. Silvester and A. Wathen, *SIAM Journal on Numerical Analysis* **31**(5), 1352–1367 (1994).
- [11] I. N. Sneddon, *Proc. Roy. Soc. London Ser. A* **187**, 229–260 (1946).
- [12] I. N. Sneddon and M. Lowengrub, *Crack problems in the classical theory of elasticity*, SIAM series in Applied Mathematics (John Wiley and Sons, Philadelphia, 1969).
- [13] T. Heister, M. F. Wheeler, and T. Wick, *Computer Methods in Applied Mechanics and Engineering* **290**, 466–495 (2015).
- [14] T. Heister and T. Wick, *Software Impacts* **6**, 100045 (2020).
- [15] D. Arndt, W. Bangerth, B. Blais, T. C. Clevenger, M. Fehling, A. V. Grayver, T. Heister, L. Heltai, M. Kronbichler, M. Maier et al., *Journal of Numerical Mathematics* **1** (2020).
- [16] M. A. Heroux, R. A. Bartlett, V. E. Howle et al., *ACM TOMS* **31**(3), 397–423 (2005).
- [17] J. Schröder, T. Wick, S. Reese et al., *Archives of Computational Methods in Engineering* **28**(2), 713–751 (2021).